

Heterogeneous Memory Pool Tuning

Filip Vaverka*, Ondrej Vysocky†, Lubomir Riha‡
IT4Innovations, VSB – Technical University of Ostrava
Ostrava-Poruba, Czech Republic

Email: *filip.vaverka@vsb.cz, †ondrej.vysocky@vsb.cz, ‡lubomir.riha@vsb.cz

Abstract—We present a lightweight tool for the analysis and tuning of application data placement in systems with heterogeneous memory pools. The tool allows non-intrusively identifying, analyzing, and controlling the placement of individual allocations of the application. We use the tool to analyze a set of benchmarks running on the Intel Sapphire Rapids platform with both HBM and DDR memory. The paper also contains an analysis of the performance of both memory subsystems in terms of read/write bandwidth and latency. The key part of the analysis is to focus on performance if both subsystems are used together. We show that only about 60 % to 75 % of the data must be placed in HBM memory to achieve 90 % of the potential performance of the platform on those benchmarks.

Index Terms—Heterogeneous Memory, HBM, NUMA.

I. INTRODUCTION

The rapidly growing per-socket compute capability of modern CPUs, fueled by large increases in core counts and the introduction of wide vector and advanced matrix instruction set extensions, puts equally rapidly growing demands on memory bandwidth. However, keeping up with these bandwidth demands increases both the complexity and the power usage of a platform. The typical mitigation strategy (increasing the amount of on-chip cache memory) may not be sufficient for notoriously data-intensive HPC applications. The advancements in packaging allow us to further alleviate this issue by including a limited amount of high-bandwidth memory on the CPU package. The typical memory of choice for this application is High-Bandwidth Memory (HBM) with a wide data bus and vertical stacking of dynamic memory dies. This memory either takes the place of traditional DDR memory (e.g., A64FX [1]) or is used as an additional cache level or manually managed scratch pad on top of the DDR memory (e.g., Intel Xeon Max Series [2]).

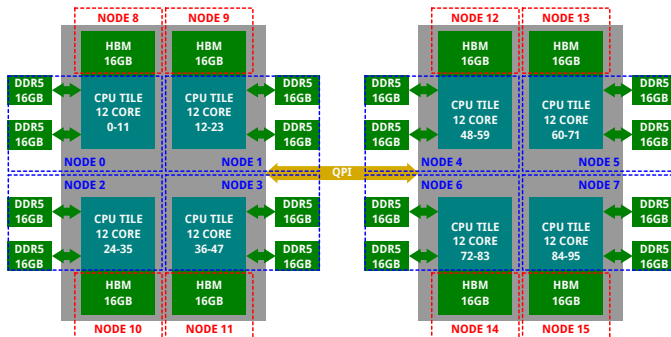


Fig. 1: NUMA architecture of dual Intel Xeon Max 9468 server in flat SC4 mode.

A. Platform Investigation

In this article, we investigate the potential of using HBM memory on a CPU package as a manually managed scratch pad on a range of basic parallel benchmarks. The platform chosen for the investigation is a machine equipped with two Intel Xeon Max 9468 CPUs (Intel Sapphire Rapids family - SPR) (see Fig. 1). The CPU is built as four tiles with EMIB interconnect between them, each of these tiles consists of 12 cores, one HBM2e memory stack (16 GB at 409.6 GB/s peak) and dual-channel DDR5 memory controller (32 GB at 76.8 GB/s peak). In practice, the CPU can achieve only about 700 GB/s and 200 GB/s respectively [3]. These values can be confirmed by the STREAM benchmark (see Fig. 2), where a single CPU of our system achieves these values when averaging over all sub-tests. The price of a higher bandwidth is often an increase in latency, and this platform is no exception. The on-package HBM has about 20 % higher memory latency compared to DDR memory in a single-core pointer chase benchmark (see Fig. 3). The pointer chase latency penalty remains largely constant all the way up to 48 active cores, as memory access parallelism is limited to a single outstanding access per core. However, the increased latency can be counteracted by the HBM bandwidth in cases with a higher degree of memory access parallelism. This can be seen in cases such as reads from known random addresses that can be issued independently of each other (see Fig. 4).

Given that we want to make the optimal use of both kinds of memory simultaneously, the final piece of the puzzle is the interaction between them. To get a rough picture, we

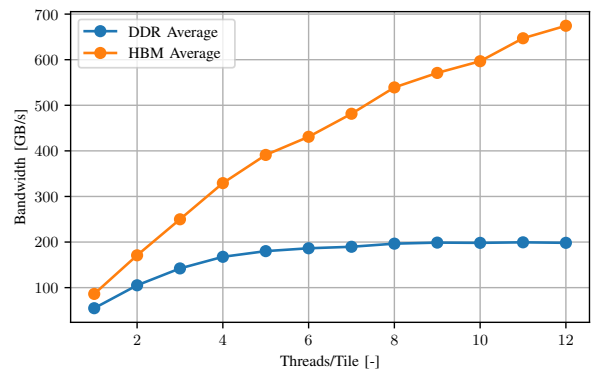


Fig. 2: Memory bandwidth measured with STREAM benchmark with all data in DDR or HBM memory.

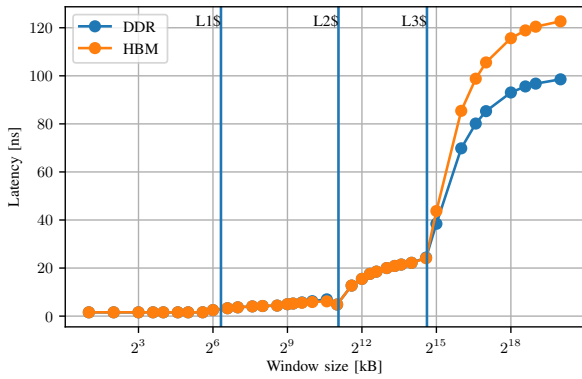


Fig. 3: The on-package HBM of Intel Xeon Max 9468 exhibits about 20 % higher latency compared to the DDR memory.

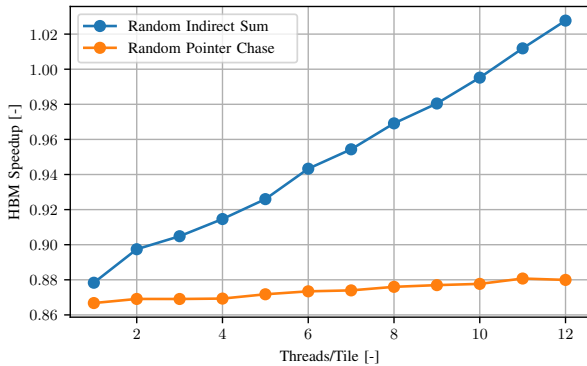
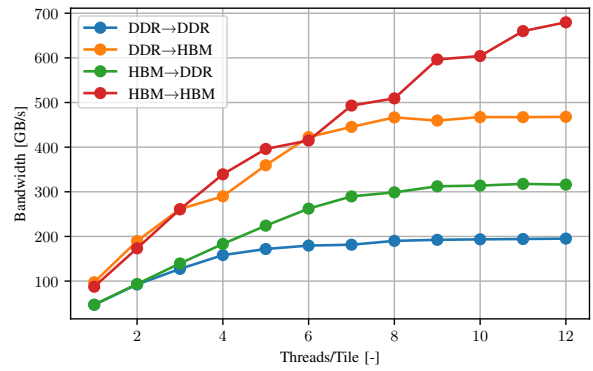


Fig. 4: Random memory access speedup for summation of randomly spaced values and random pointer chase in 32 GB array uniformly spread over all DDR or HBM memory nodes of a single socket. Speedup below one means DDR memory is faster than HBM.

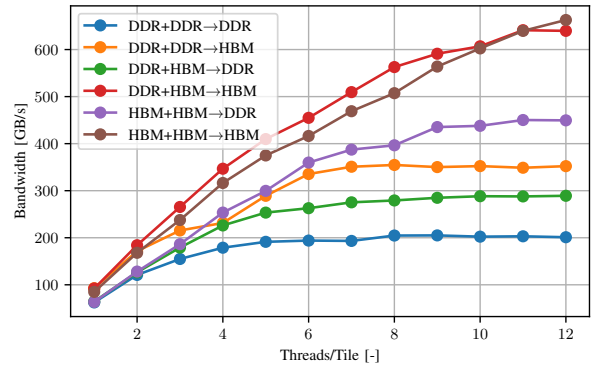
return to the STREAM benchmark, but instead of binding the whole application to a particular memory pool, we distribute allocations individually. Figure 5 shows the bandwidth scaling of STREAM’s *Copy* and *Add* sub-tests for each data placement configuration.

While the cases where all the data are placed in DDR or HBM memory pools reflect the peak bandwidth of respective memory pools, the situation is more interesting for mixed cases. The copy kernel performs considerably worse when copying from HBM to DDR memory than the other way around (see Fig. 5a), achieving only about 65 % of expected bandwidth. The behavior is similar for the Add kernel, where reading two arrays from HBM memory and writing the result to DDR memory (HBM + HBM→DDR) performs similarly to its complementary configuration (DDR + DDR→HBM). On the other hand, we can achieve HBM-only performance while storing one of the input arrays in DDR memory (saving a third of the limited HBM memory capacity).

These results suggest that there may be some potential for data placement optimization in more complex applications. Potential latency penalties may be alleviated by moving as-



(a) STREAM: Copy



(b) STREAM: Add

Fig. 5: Memory bandwidth of Copy and Add sub-tests of STREAM benchmark in relation to placement (DDR or HBM) of each work array (16 GB per array).

sociated allocations back to DDR memory, or HBM memory usage may be reduced at minimal performance cost.

II. RELATED WORK

The problem of application data placement in systems with heterogeneous memory can be tackled from a software point of view at a memory page or an allocation (object) granularity. Regardless of the chosen granularity, the system typically consists of three main components: memory usage analysis (profiling), placement algorithm, and data placement control tool or library.

The memory page granularity approach can be implemented at the OS (e.g. [4], [5]) or even at the hardware level. These systems typically rely on page access patterns and statistics to make decisions on page placement. While this approach allows the system to be fully transparent to the application, it is often limited to reactive data movement.

The object-level approaches no longer treat the application as a black box and analyze its data in terms of logical objects or allocations. This allows to analyze usage patterns for each object created by the application and proactively plan placement of these objects for subsequent runs of the application. The analysis is typically performed separately using various combinations of simulation, instrumentation (e.g., tools built

on top of Intel PIN [6] or DynamoRIO [7]), and profiling (using hardware counters and instruction-based sampling such as AMD IBS [8] or Intel PEBS [9]). Laghari et al.[10] used the ADAMANT [11] tool to collect performance data to demonstrate their proposed object placement algorithm on the Intel Knights Landing (KNL) platform. The ADAMANT tool uses a combination of all three to collect the data. Similarly, ecoHMEM [12] uses Extrae [13] to collect object statistics as the first step and FlexMalloc [14] to control the placement of objects according to the precomputed plan.

III. METHODOLOGY

Our approach (see Fig. 6) attempts to take the first step towards a more dynamic approach, which combines both allocation analysis and control in a single tool and potentially allows for online profiling and control. Our tool instruments individual allocations and uses CPU performance counters (through Linux perf API [15]) in combination with instruction-based sampling (IBS). The allocation instrumentation can be performed by overriding memory management calls using *shim library* or recompiling the application when necessary. This allows us to precisely track the lifetime of each allocation and correlate it with the source code location using a stack trace of the call. The intercepted allocation call can also be overridden to allocate from a specific memory pool (such as HBM or DDR). The combination of IBS with known allocation address range allows us to estimate the density and other statistics (latency, cache hit rate, etc.) of memory accesses into each allocation.

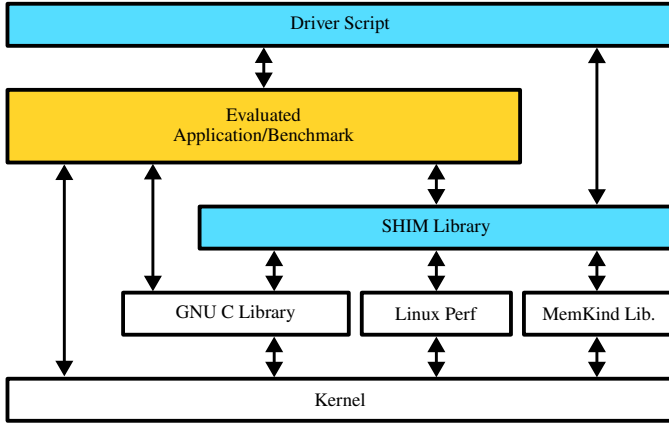


Fig. 6: The presented analysis and tuning tool consists of driver script and SHIM library (blue). The driver script collects statistics, while the SHIM library overrides memory allocations based on a plan constructed by the driver script.

This approach allows for the minimization of the overhead of the instrumentation, as memory allocations should not be performed in the critical path of the application while gathering helpful information for both the developers of the application and the automatic tuning tool. One of the limitations of using stack traces to identify allocations is the inability to easily distinguish between allocations in subsequent loop iterations.

A. Measurement and Analysis

For our purposes, the application can be viewed as a fixed workload and its working data set as a set of individual allocations $A_R = \{a_1, a_2, \dots, a_n\}$. The set of allocations A_R together with the set of available physical memory pools $P = \{p_1, p_2, \dots, p_m\}$ defines our complete configuration space. The metric of interest is the performance of the application (with fixed workload) as the mapping of the allocations (A_R) to the memory pools (P) changes. The set of all possible mappings C from A_R to P can be enumerated as $C = \{c \mid c \in \mathbb{P}(A_R)^P \wedge \bigcup c = A_R \wedge c_i \cap c_j = \emptyset \text{ for } i \neq j\}$, which is the set of tuples where the element c_i is a set of allocations placed into the memory pool $p_i \in P$.

In practice, the tooling captures only a subset of allocations $A_C \subseteq A_R$ due to the aliasing of stack traces discussed in the previous section. The aliased allocations are treated as a single allocation (i.e., these allocations will always be placed into the same memory pool). The captured allocations A_C are further filtered and possibly grouped to restrict configuration space C and thus analysis time. Typically, allocations smaller than L2 or L3 cache size can be assumed to be insignificant and are ignored or folded into a single allocation group. For the purposes of this article, we decided to aim for 8 allocation groups, which are chosen as the top 7 allocations (when ranked by individual performance impact), while the rest are included in the last group.

Taking into account only two available memory pools on our platform (DDR and HBM), the configuration space on the allocation groups A_G can be written as $C = \{(\bigcup x, A_C \setminus \bigcup x) \mid x \in \mathbb{P}(A_G)\}$, where A_G is some partition of A_C . This leaves us with roughly $2^{|A_G|}n$ measurements (averaging over n runs for each configuration) needed to characterize the application sufficiently (given a fixed workload).

Figure 7 shows two views of the results for the analysis of the NPB Multi-Grid benchmark application. This benchmark has in total three significant allocations (see the left-most section of Fig. 7a) of similar size, roughly 1/3 of overall memory (26.5 GB) used by the benchmark. Each of these three allocations also has associated relative memory access density determined as fraction of all memory accesses (sampled using IBS/PEBS) falling in the address range of the allocation. The first two allocation groups (0 and 1) together comprise more than 90% of all memory access samples, and moving either of them into the HBM memory pool yields more than 1.6 \times speedup. Moving both of those allocations into HBM at the same time allows to achieve more than 2.2 \times speedup. The expected speedup is computed as linear combination of speedup achieved by each allocation group individually (i.e., allocation groups are assumed to be independent). The middle and right sections of Fig. 7a show the same information for pairs and the three allocation groups, respectively.

Figure 7b offers a more concise view of the same data but skips information on the impact of individual combinations of allocation groups and associated memory access densities.

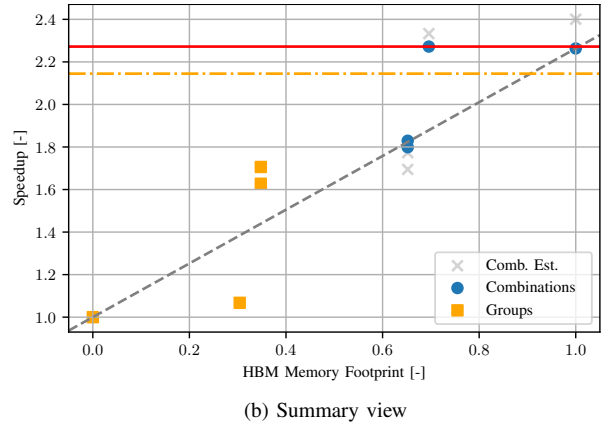
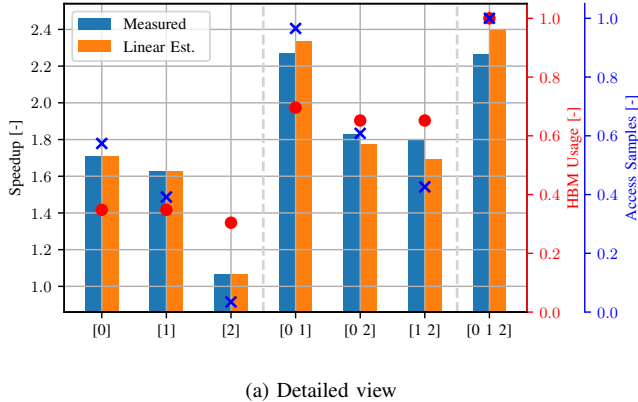


Fig. 7: Analysis of the Multi-Grid benchmark of the NAS Parallel Benchmark Suite (NPB) for all possible placements of significant allocations. The detailed view (Fig. 7a) shows 3 allocations in 7 DDR/HBM placement configurations (DDR-only placement is used as a reference for speedup). The bars denote measured (blue) and expected (orange) speedup of each configuration, while red dots and blue crosses denote fraction of the data in HBM and fraction of memory accesses to the data in HBM (IBS/PEBS sampled) respectively.

The summary view (Fig. 7b) focuses exclusively on the relationship between speedup and fraction of the application data in HBM. The results are shown as scatter plot with yellow squares denoting results for individual allocations in HBM plus the DDR-only case, while blue dots denote combinations of two or more allocations in HBM (corresponding to blue bars in Fig. 7a). The gray crosses show expected speedup (corresponding to orange bars in Fig. 7a). Finally, the horizontal lines denote the maximum (solid red line) and 90% of the maximum (dash-dotted orange line) speedup.

However, it provides a better overview of the overall relationship between the amount of data in HBM memory and the performance of the application. In the case of NPB: Multi-Grid benchmark, Figure 7b shows that there exists memory pool assignment, which achieves maximum speedup (solid red line) with only 70% of the data in the HBM memory pool, and moving the rest of the data from DDR to HBM does not bring any further improvement.

IV. RESULTS

We illustrate the capabilities of the tool on selected benchmarks from the OpenMP version of the well-known NAS Parallel Benchmark suite (NPB [16]) and k-Wave [17], a widely used ultrasound propagation solver for medical applications. The benchmark configurations (see Table I) are chosen so that enough memory is used (about 8 GB to 30 GB) to avoid cache effects (which would not apply in case of realistic application runs) while runtime of each benchmark is kept short enough. For these reasons, we also slightly reduced the number of iterations for iterative benchmarks, as a shorter runtime is sufficient for comparative use.

The Integer Sort benchmark was modified by disabling blocking (which optimizes for cache efficiency) and increasing the size of its work set.

A. NAS Parallel Benchmarks

The arithmetic intensity (see Fig. 8) is a good starting point to estimate the performance gain achievable by taking advantage of HBM. The STREAM Add, and Triad kernels are included to put our memory traffic estimation in context.

TABLE I: Benchmarks used to evaluate the proposed tool, their configuration and properties.

Application	Benchmark Variant	Memory Usage [GB]	Filtered Allocations
NPB: Multi-Grid	mg.D	26.46	3
NPB: Block Tri-diag.	bt.D	10.68	9
NPB: Lower-Upper GS.	lu.D	8.65	7
NPB: Scalar Penta-diag.	sp.D	11.19	10
NPB: Unst. Adapt. Mesh	ua.D	7.25	56
NPB: Integer Sort (NB)	is.C*	20	4
k-Wave Solver 512 ³ Grid	-	9.79	34

The roofline model suggests that Multi-Grid (Fig. 9) and Unstructured Adaptive Mesh (Fig. 10) benchmarks should benefit the most from HBM memory due to their low arithmetic intensity. Although Multi-Grid can achieve its maximum speedup (2.27 \times) with only 69.6% of the data in the HBM, the Unstructured Adaptive Mesh Solver achieves only a maximum of 1.49 \times with similar 68.8% of its data in HBM. However, in the latter case, a nearly similar performance can be achieved already with less than 60% of the data in the HBM.

Although Scalar Penta-diagonal Solver has considerably higher arithmetic intensity (at least when it comes to the DRAM bandwidth), it exhibits slightly higher maximum speedup of 1.79 \times and 1.70 \times at 68.8% of the data in HBM (see Fig. 11).

Both Block Tri-diagonal Solver (see Fig. 12) and Lower-Upper Gauss-Seidel Solver (see Fig. 13) achieve only modest peak speedup of 1.15 \times and 1.27 \times , respectively. However, the

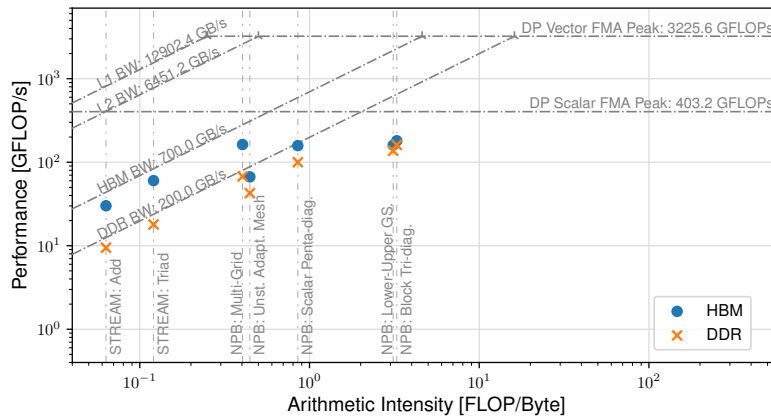


Fig. 8: Estimated roofline model of a single Intel Xeon Max 9468 CPU (at 2.1 GHz base clock). The arithmetic intensity is roughly estimated from the number of memory read requests fulfilled by DRAM.

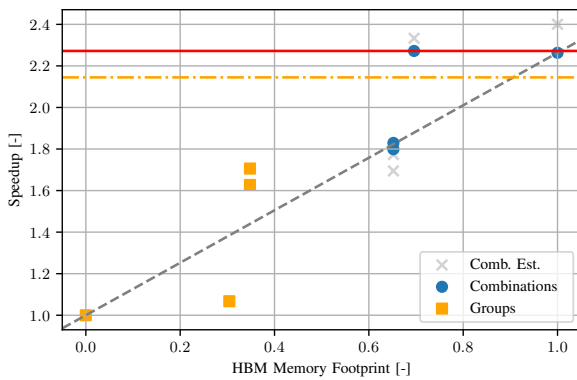


Fig. 9: Summary view for NPB: Multi-Grid Solver

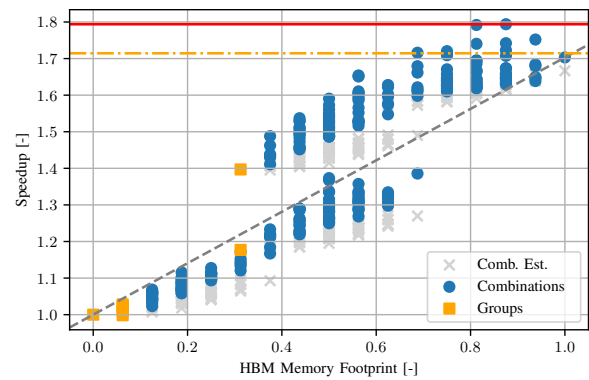


Fig. 11: Summary view for NPB: Scalar Penta-diagonal Solver

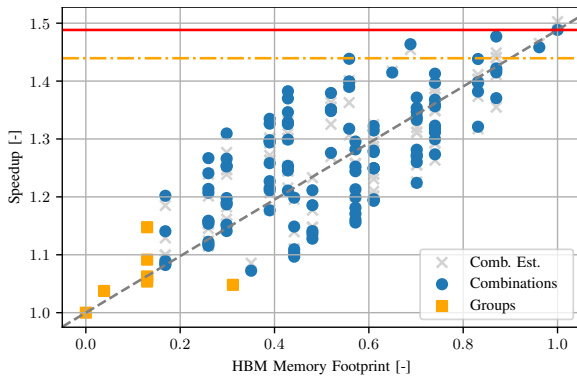


Fig. 10: Summary view for NPB: Unstructured Adaptive Mesh Solver

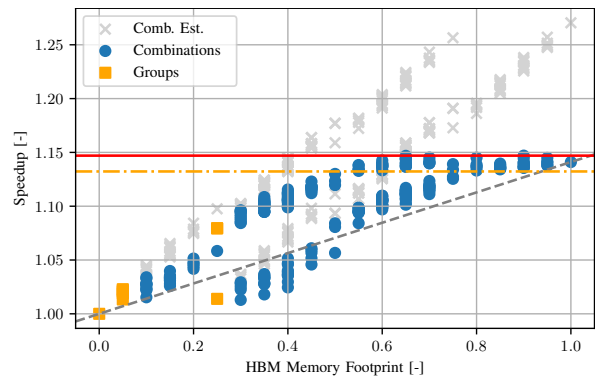


Fig. 12: Summary view for NPB: Block Tri-diagonal Solver

90% speedup at around 60% of the data in HBM still holds for both benchmarks. Interestingly, most of the speedup of the Lower-Upper Gauss-Seidel Solver can be achieved by moving a single allocation (which comprises only about 25% of the memory footprint) to HBM memory.

The “Integer Sort” (see Fig. 14) achieves the maximum speedup of 2.21 \times , although it is supposed to test random

memory access, which can be affected by the higher memory latency of HBM.

B. *k-Wave Solver*

Finally, *k-Wave* [17] is a pseudospectral solver for non-linear sound wave propagation and heavily relies on the Fast Fourier Transform over 3D complex-valued arrays. The rest of the working arrays are similarly structured so that three allocations comprise a single vector field in three spatial

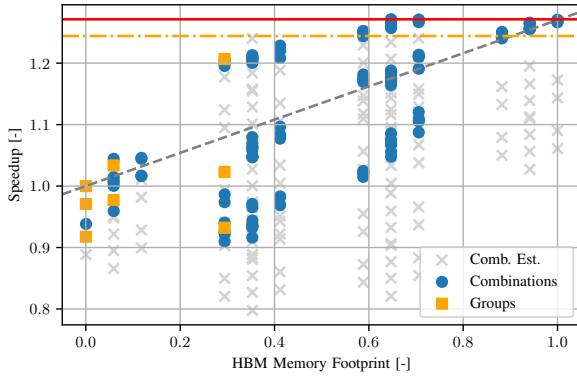


Fig. 13: Summary view for NPB: Lower-Upper Gauss-Seidel Solver

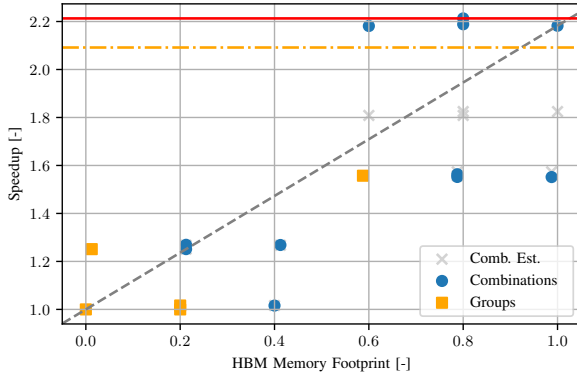


Fig. 14: Summary view for NPB: Integer Sort

dimensions. Therefore, we chose an allocation grouping that reflects this, and the arrays for each vector field are considered a single allocation group. The complex-valued arrays for 3D FFTs are kept separately as these have the most impact on their own.

The application achieves a speedup of $1.32\times$, and although complex-valued arrays have the most impact, more than $3/4$ of the data must be placed in HBM to achieve 90% speedup. The requirement to place more data (compared to the benchmarks) in the fast memory to achieve 90% speedup can be, at least partially, accounted for by k-Wave being already carefully optimized for the small memory footprint.

V. CONCLUSION

In this article, we introduce a simple tool for analyzing the memory usage of applications on platforms with multiple diverse memory pools. The tool can provide helpful information, such as the usage and performance impact of moving individual allocations between these memory pools. This information can be used by the developer or the tuning tool to optimize mapping between application data and memory pools, thus allowing for efficient use of fast memory of limited size (such as HBM of the SPR platform).

Table II summarizes the results collected for the selected benchmarks. Although the latency penalty of HBM did not

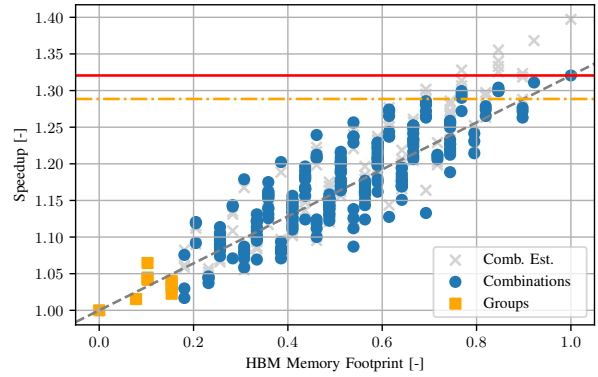


Fig. 15: Summary view for k-Wave 512^3 Grid

TABLE II: Summary of the results achieved by the proposed tool on the selected benchmarks.

Application	Maximum Speedup [-]	HBM-only Speedup [-]	90% Speedup HBM Usage [%]
NPB: Multi-Grid	2.27	2.26	69.6
NPB: Block Tri-diag.	1.15	1.14	55.0
NPB: Lower-Upper GS.	1.27	1.27	58.8
NPB: Scalar Penta-diag.	1.79	1.70	68.8
NPB: Unst. Adapt. Mesh	1.49	1.49	68.8
NPB: Integer Sort (NB)	2.21	2.18	60.0
k-Wave Solver 512^3 Grid	1.32	1.32	76.8

prove to be sufficient to warrant keeping some of the data of these applications in DDR memory, we have shown that 25% to 30% can be kept in DDR memory while maintaining near-peak performance.

ACKNOWLEDGMENTS

This work was supported by the Ministry of Education, Youth and Sports of the Czech Republic through the e-INFRA CZ (ID:90254).

This work was supported by the MaX project under grant agreement No 101093374. The project is supported by the European High-Performance Computing Joint Undertaking and its members (including top-up funding by the Ministry of Education, Youth and Sports of the Czech Republic ID: MC2303).

REFERENCES

- [1] T. Yoshida, "Fujitsu high performance cpu for the post-k computer," in *Hot Chips: A Symposium on High Performance Chips*, 2018. [Online]. Available: https://old.hotchips.org/hc30/2conf/2.13_Fujitsu_HC30_Fujitsu.Yoshida.rev1.2.pdf.
- [2] *Intel® xeon® cpu max series*, 2024. [Online]. Available: <https://www.intel.com/content/www/us/en/products/details/processors/xeon/max-series.html>.

- [3] J. D. McCalpin, “Bandwidth limits in the intel xeon max (sapphire rapids with hbm) processors,” in *High Performance Computing*, A. Bienz, M. Weiland, M. Baboulin, and C. Kruse, Eds., Cham: Springer Nature Switzerland, 2023, pp. 403–413, ISBN: 978-3-031-40843-4.
- [4] W. Zhang and T. Li, “Exploring phase change memory and 3d die-stacking for power/thermal friendly, fast and durable memory architectures,” in *2009 18th International Conference on Parallel Architectures and Compilation Techniques*, Raleigh, North Carolina, USA: IEEE, Sep. 2009, pp. 101–112, ISBN: 978-0-7695-3771-9. DOI: 10.1109/PACT.2009.30. [Online]. Available: <http://ieeexplore.ieee.org/document/5260554/> (visited on 03/12/2025).
- [5] F. X. Lin and X. Liu, “memif: Towards programming heterogeneous memory asynchronously,” in *Proceedings of the Twenty-First International Conference on Architectural Support for Programming Languages and Operating Systems*, Atlanta Georgia USA: ACM, Mar. 25, 2016, pp. 369–383, ISBN: 978-1-4503-4091-5. DOI: 10.1145/2872362.2872401. [Online]. Available: <https://dl.acm.org/doi/10.1145/2872362.2872401> (visited on 03/12/2025).
- [6] C.-K. Luk, R. Cohn, R. Muth, *et al.*, “Pin: Building customized program analysis tools with dynamic instrumentation,” in *Proceedings of the 2005 ACM SIGPLAN Conference on Programming Language Design and Implementation*, ser. PLDI ’05, Chicago, IL, USA: ACM, 2005, pp. 190–200, ISBN: 1-59593-056-6. DOI: 10.1145/1065010.1065034. [Online]. Available: <http://doi.acm.org/10.1145/1065010.1065034>.
- [7] D. Bruening, Q. Zhao, and S. Amarasinghe, “Transparent dynamic instrumentation,” in *Proceedings of the 8th ACM SIGPLAN/SIGOPS Conference on Virtual Execution Environments*, ser. VEE ’12, London, England, UK: ACM, 2012, pp. 133–144, ISBN: 978-1-4503-1176-2. DOI: 10.1145/2151024.2151043. [Online]. Available: <http://doi.acm.org/10.1145/2151024.2151043>.
- [8] *Amd64 architecture programmer’s manual*, 2024. [Online]. Available: <https://www.amd.com/content/dam/amd/en/documents/processor-tech-docs/programmer-references/40332.pdf>.
- [9] *Intel® 64 and ia-32 architectures software developer’s manual*, 2024. [Online]. Available: <https://www.intel.com/content/www/us/en/content-details/843820/intel-64-and-ia-32-architectures-software-developer-s-manual-combined-volumes-1-2a-2b-2c-2d-3a-3b-3c-3d-and-4.html>.
- [10] M. Laghari and D. Unat, “Object placement for high bandwidth memory augmented with high capacity memory,” in *2017 29th International Symposium on Computer Architecture and High Performance Computing (SBAC-PAD)*, Campinas: IEEE, Oct. 2017, pp. 129–136, ISBN: 978-1-5090-1233-6. DOI: 10.1109/SBAC-PAD.2017.24. [Online]. Available: <http://ieeexplore.ieee.org/document/8102187/> (visited on 03/10/2025).
- [11] P. Cicotti and L. Carrington, “ADAMANT: Tools to capture, analyze, and manage data movement,” *Procedia Computer Science*, vol. 80, pp. 450–460, 2016, ISSN: 18770509. DOI: 10.1016/j.procs.2016.05.323. [Online]. Available: <https://linkinghub.elsevier.com/retrieve/pii/S1877050916307189> (visited on 03/10/2025).
- [12] M. Jorda, S. Rai, E. Ayguade, J. Labarta, and A. J. Pena, “ecoHMEM: Improving object placement methodology for hybrid memory systems in HPC,”
- [13] *Extrae*, Barcelona Supercomputing Center, 2024. [Online]. Available: <https://tools.bsc.es/extrae>.
- [14] H. Servat, *Flexible memory allocation tool for multi-tiered memory systems*, 2024. [Online]. Available: <https://github.com/intel/flexmalloc>.
- [15] *Perf: Linux profiling with performance counters*, 2024. [Online]. Available: <https://perfwiki.github.io/main>.
- [16] *Nas parallel benchmarks*, 2024. [Online]. Available: <https://www.nas.nasa.gov/software/npb.html>.
- [17] J. Jaros, A. P. Rendell, and B. E. Treeby, “Full-wave nonlinear ultrasound simulation on distributed clusters with applications in high-intensity focused ultrasound,” *International Journal of High Performance Computing Applications*, vol. 30, no. 2, pp. 137–155, 2016.